Biochimica et Biophysica Acta, 936 (1988) 361–371
Elsevier

BBA 42889

Determination of free energies in reaction centers of *Rb. sphaeroides*

A. Ogrodnik [a], M. Volk [a], R. Letterer [a], R. Feick [b] and M.E. Michel-Beyerle [a]

[a] *Institut für Physikalische und Theoretische Chemie, Technische Universität München, Garching and* [b] *Max-Planck-Institut für Biochemie, Martinsried (F.R.G.)*

(Received 26 February 1988)
(Revised manuscript received 30 May 1988)

Key words: Free energy difference; Reaction center; Photosynthesis; Radical pair lifetime; Magnetic field effect; (*Rb. sphaeroides*)

Magnetic field-dependent recombination measurements together with magnetic field-dependent triplet lifetimes (Chidsey, E.D., Takiff, L., Goldstein, R.A. and Boxer, S.G. (1985) Proc. Natl. Acad. Sci USA 82, 6850–6854) yield a free energy change $\Delta G(P^+H^- - {}^3P^*) = 0.165$ eV ± 0.008 at 290 K. This does not depend on whether nuclear spin relaxation in the state $^3P^*$ is assumed to be fast or slow compared to the lifetime of this state. This value, being (almost) temperature independent, indicates $\Delta G(P^+H^- - {}^3P^*) \simeq \Delta H(P^+H^- - {}^3P^*)$ and is consistent with $\Delta G({}^1P^* - P^+H^-)$ and $\Delta H({}^1P^* - {}^3P^*)$ from previous delayed fluorescence and phosphorescence data, implying $\Delta G \simeq \Delta H$ for all combinations of these states.

Introduction

The primary electron transfer process in reaction centers (RCs) of *Rb. sphaeroides* proceeds from the bacteriochlorophyll dimer in its excited singlet state ($^1P^*$) to bacteriopheophytin (H) forming the radical pair (RP) state P^+BH^- with a rate $k_1 = 3.6\ 10^{11}\ s^{-1}$ [1] at room temperature. Femto- and picosecond time-resolved spectroscopy excludes any kinetic involvement [2–4] of the accessory bacteriochlorophyll (B) located between P and H as revealed in the X-ray structure analysis [5–7]. A complementary experimental key to the mechanism of the primary charge separation is the magnetic-field-dependent recombination dynamics of P^+BH^- [8–10] leading to either the triplet state ($^3P^*$) or the ground state (PBH). For any mechanistic interpretation [11–15] of the forward and the reverse electron transfer rates, the free energy difference ΔG between $^1P^*$ and P^+BH^- and between P^+BH^- and $^3P^*$ is essential.

Recombination of P^+BH^- occurs when electron transfer between H and the ubiquinone is blocked, e.g., by extraction of the quinone (Q). In this case the RP initially formed in its singlet state $^1(P^+BH^-)$ undergoes singlet-triplet mixing under the influence of hyperfine interaction (HFI), yielding the triplet-phased RP $^3(P^+BH^-)$. Recombination of $^3(P^+BH^-)$ into the state $^3P^*$ with the rate k_T competes with recombination of $^1(P^+BH^-)$ leading to the ground state (PBH) with the overall singlet rate k_S. This rate k_S has a contribution from direct recombination into the ground state as well as a contribution involving recombination into $^1P^*$, a minor part of which can subsequently deactivate into the ground state, while the gross

Abbreviations: RC, reaction center; RP, radical pair; HFI, hyperfine interaction; LDAO, lauryldimethylamine *N*-oxide, SLR, spin lattice relaxation.

Correspondence: M.E. Michel-Beyerle, Institut für Physikalische und Theoretische Chemie, Technische Universität München, Lichtenbergstr. 4, 8046 Garching, F.R.G.

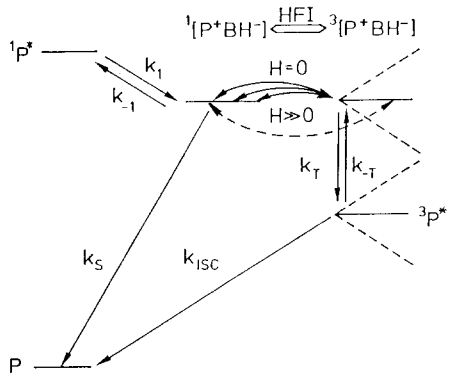

Fig. 1. Reaction scheme for charge separation and recombination of singlet and triplet excited states connected via the RP mechanism.

majority forms again the RP $^1(P^+BH^-)$. The energy splitting between the singlet and the triplet RP states, as indicated in Fig. 1, impedes HFI-induced singlet–triplet mixing. This allows the manipulation of the singlet and triplet recombination yields by splitting the triplet levels via Zeeman interaction in an external magnetic field (H).

The observation of a magnetic field dependence of the thermally activated contributions to the observed $^3P^*$ decay rates [16] points to a decay path of $^3P^*$ in addition to conventional intersystem crossing. This magnetic field dependence is qualitatively the same as for the radical pair lifetimes, being sensitive to rather small magnetic fields, a feature exclusively typical of the radical pair mechanism. In fact, it proves an additional pathway to be operative, involving temperature-activated back-transfer of the electron to form $^3[P^+BH^-]$ with the rate k_{-T}, HFI-induced formation of $^1(P^+BH^-)$ (this step being magnetic-field dependent) and final decay to PBH with the rate k_S.

From the magnetic field dependence of the $^3P^*$ lifetimes reported by Chidsey et al. [16], together with the magnetic field dependence of the triplet yield and the knowledge of the parameters k_s and k_T, the rate k_{-T} is evaluated at various temperatures. Temperature-dependent measurements of the remaining parameters are presented. The ratio k_{-T}/k_T allows the determination of the free energy difference $\Delta G(RP - {}^3P^*)$ at different temperatures. The result is related to $\Delta G(^1P^* - RP)$ and $\Delta G(^1P^* - {}^3P^*)$ as derived from delayed fluorescence [17–19] and to the recent phosphorescence data [20] yielding $\Delta H(^1P^* - {}^3P^*)$. All these data and others mentioned throughout the text refer to quinone-depleted RCs of *Rb. sphaeroides* R26, if not explicitly stated otherwise. In particular, we caution against mixing such data with those obtained from RCs blocked by quinone reduction.

Analysis of magnetic-field-dependent triplet lifetimes

In the simplest model (a) the distribution of nuclear spins is neglected and only one representative HFI coupling constant is considered. Such an analysis described in the following shows the basic relations most clearly. A more realistic analysis will account for the effects of the statistical alignment of nuclear spins as an inhomogeneous distribution of RCs with different effective HFI coupling constants [21,22]. As has been discussed in Ref. 22 the observed triplet lifetime may depend on the nuclear spin lattice relaxation (SLR) time. Since we have no knowledge of its value, we analyse our data assuming two extreme cases: (b) nuclear SLR being (infinitely) slow, and (c) nuclear SLR being (infinitely) fast as compared to the triplet lifetime. In this way we obtain two sets of data (b) and (c) embracing the real value, respectively.

Model neglecting nuclear spin distribution

After charge separation the initially formed RP $^1(P^+BH^-)$ has a time-integrated probability, Π_T, to form the triplet state $^3(P^+BH^-)$ due to singlet–triplet mixing [23]. This state subsequently recombines with the rate k_T to the lowest triplet state of the system, $^3P^*$. Its yield is given by $\Phi_T = k_T \Pi_T$ and implies the recombination yield in the singlet channel, being $\Phi_S = 1 - \Phi_T$. The magnetic field removes the degeneracy between the singlet level and two of the triplet sublevels, thus reducing the mixing efficiency, Π_T, and consequently also Φ_T.

If the RP is repopulated by charge separation from $^3P^*$ with the rate k_{-T}, the triplet state $^3(P^+BH^-)$ is the initially formed spin state of the RP. Following a suitable treatment of radical pair

spin dynamics [23], the relation $\Pi_S = \Pi_T/3$ has been derived [16], where Π_S is the time-integrated probability for the change from $^3(P^+BH^-)$ to $^1(P^+BH^-)$, which can be expressed by Φ_T and k_T, both quantities being accessible in experiments. The fraction, Φ_S', of the initially populated $^3(P^+BH^-)$ state, which changes multiplicity and recombines to the electronic ground state PBH, is given by $\Phi_S' = k_S \Pi_S$. The product of this fraction with the rate k_{-T} yields the decay rate of $^3P^*$ via $^3(P^+BH^-)$. Since Π_S can be expressed by Π_T and thus in terms of the experimentally accessible quantities Φ_T and k_T, the overall decay rate of $^3P^*$, k_{DEC} is given by [16]:

$$k_{DEC}(H) = k_{ISC} + \tfrac{1}{3}\frac{k_S}{k_T}\Phi_T(H)k_{-T} \tag{1}$$

with k_{ISC} denoting the rate of intersystem crossing $^3P^* \rightarrow P$.

Alternatively to Ref. 16, we take advantage of the magnetic field dependence of k_{DEC} and of Φ_T to eliminate k_{ISC} from Eqn. 1. The rate k_{-T} for the charge separation from $^3P^*$ is expressed by the difference of these parameters when changing the magnetic field from H_1 to H_2:

$$k_{-T} = \frac{k_{DEC}(H_1) - k_{DEC}(H_2)}{\Phi_T(H_1) - \Phi_T(H_2)} \frac{3k_T}{k_S} \tag{2}$$

Model including nuclear spin distribution

As pointed out in Refs. 21, 22, we are dealing with an inhomogeneous distribution of RCs with respect to the nuclear spin configuration of each individual RC. To account for the consequences of such an inhomogeneous distribution on the triplet lifetime, we follow the approach given in Ref. 22. Each nuclear spin configuration corresponds to a different effective HFI coupling constant ω with a distribution $R^0(\omega, H)$. The second variable, H, indicates that the distribution depends on whether a magnetic field is applied or not (Eqn. 4 or 6, respectively in Ref. 22). Those RCs with nuclear spins alligned parallel feel a stronger effective hyperfine interaction (large ω) driving singlet–triplet mixing and achieve a higher triplet recombination yield than RCs in which the hyperfine contributions of the various nuclei cancel. This means the triplet evolution is selective to the larger HFIs leading to nuclear spin polarization of the $^3P^*$ state. Instead of the equilibrium distribution of HFIs, the new distribution is given by Eqn. 3 (Ref. 22):

$$R^3(\omega, H) = \Phi_T(\omega, H) R^0(\omega, H) \tag{3}$$

As emphasized in Ref. 22, the apparent (or observed) triplet lifetime $1/k_{OBS}$ of the inhomogeneous distribution can be obtained by averaging over the individual decaytimes $1/k_{DEC}$ given in Eqn. 1.

$$\frac{1}{k_{OBS}(H)} = \frac{\int R^3(\omega, H)\, d\omega / k_{DEC}(\Phi_T(\omega, H))}{\int R^3(\omega, H)\, d\omega} \tag{4}$$

Since $\Phi_T(\omega)$, the triplet yield as a function of the hyperfine field, is no more experimentally observable, we utilize Eqns. 7 and 8 of Ref. 23. The linear relationship between k_{DEC} and the triplet yield in Eqn. 1, in general, breaks down. Only in the case of extremely high magnetic fields ($\Delta g \beta H \gg$ HFI), when singlet–triplet mixing would be dominated by the difference in g values ($\Delta g \approx -1 \cdot 10^{-3}$ [24]) of the two radical ions, P^+ and H^-, can the integration over the distribution of HFI coupling constants be formally neglected. Then, however, attention should be paid to the anisotropy of the g values [24]. As in the simple approach leading to Eqn. 2, we again make use of the magnetic field modulation of both the triplet yield and the observed triplet lifetime to determine the two unknown rates, k_{-T} and k_{ISC}. Eqn. 4 given at the two field values 0 G and 700 G provides two equations for k_{OBS}, thus allowing the determination of k_{-T} and k_{ISC} by a least-squares fit of the experimental data to Eqn. 4 with a Marquardt algorithm. This method implicitly assumes that nuclear SLR is not effective throughout the triplet lifetime. Data derived under the assumption of such slow SLR are listed in Table I under (b).

If during the lifetime of $^3P^*$ the spin polarization accumulated on this state decays due to nuclear SLR, the effective HFI decreases on aver-

age and thus triplet–singlet mixing becomes increasingly slower. In the limiting case that nuclear SLR is much faster than the triplet decay, the spin distribution is equilibrated instantaneously, and we merely have to use the equilibrium distribution, R°, instead or R^3 in Eqn. 4. Data derived from such an assumption are subsequently listed in Table I under (c). Note that microscopic reversibility of the singlet–triplet transition (and vice versa) is now broken for each ensemble of RCs with a distinct nuclear configuration, due to the fast SLR occurring between the two transitions, in contrast to the situation when SLR is slow. In Ref. 22, Eqn. 1 is used to describe the case of fast SLR, tacitly assuming that the averaging procedure implicit in Eqn. 4 is equivalent to averaging the triplet yields $\Phi_T(H, \omega)$ (by measurement) before inserting into Eqn. 1. Since both averaging procedures are quite different, comparison of cases (a) and (b) is not adequate to distinguish between fast and slow SLR. In addition, only case (c) takes account for the irreversibility of SLR. For this reason we compare cases (b) and (c) with respect to the influence of SLR, both accounting in the same way for the inhomogeneity in the nuclear spin distribution.

For the evaluation of k_{-T} the experimental derivation of temperature-dependent values for $\Phi_T(H)$, k_S and k_T will be presented in the following.

Temperature- and magnetic-field dependent recombination measurements

Materials and Methods

Phototrophically grown cells of *Rhodobacter sphaeroides* R26 were used for RC isolation. Chromatophores, isolated by standard preparation procedure, were suspended in 20 mM Tris (pH 8.0) to an absorbance of 50 at 860 nm. This suspension was treated with lauryldimethylaminoxide (LDAO), 0.5% final concentration, and 100 mM NaCl for 60 min at room temperature, followed by ultracentrifugation (200 000 × *g*, 100 min). The resulting supernatant was directly applied onto a DEAE-cellulose column and subsequently washed with increasing concentrations of NaCl (110 mM + 155 mM) in 20 mM Tris/0.08% LDAO (pH 8.0). Pure RC were eluted at 190 mM NaCl concentration.

For quinone removal, dialyzed RCs were adsorbed onto a second DEAE column and subsequently treated with 2 l quinone extraction buffer (10 mM Tris/4% LDAO/10 mM *o*-phenanthroline) at 22°C. After reequilibrating the column with 20 mM Tris/0.1% Nonidet P40 (pH 8.0), RC elution was affected by 200 mM NaCl. After dialysis, RCs were concentrated to about 160 μM by ultrafiltration.

Pump and probe experiments were performed with two dye lasers (pulse width 1.4 ns) being pumped by a N_2-laser. The concentration, c_0, of quinone-depleted RCs of *Rb. sphaeroides*, R26 (50% vol. glycerol) was adjusted to give an absorbance of 0.5 at the detection wavelengths (pathlength $d = 2$ mm). The samples were excited at 600 nm with an energy density of 0.5 mJ/cm^2, corresponding to an excitation yield of $\Phi_{EXC} =$ 30% excited RCs/pulse. Time-dependent absorption changes, ΔA_P, were detected in the Q_y transition of P around 880 nm between 0 and 92 ns after excitation. Measurements were performed at zero magnetic field and at the saturating field strength of 700 G in the temperature range 295–90 K.

Since a small fraction of RCs still contain residual quinone, there may be a contribution ΔA_Q to ΔA_P due to the state P^+BHQ^-. Because of the long lifetime of this state, it can easily be discriminated from the nanosecond components. We measured the 100 ms decay of such residual bleaching at 880 nm in situ with the pulsed laser by applying a pulse sequence of one excitation pulse, followed by five probing pulses at the maximum repetition rate (15 Hz) of the system. The contribution of the 100 ms component at very short times, ΔA_Q, was extrapolated from this measurement and subtracted from ΔA_P (see Eqn. 5), leaving the light-induced absorption changes due to the Q-depleted RCs only.

On the time-scale of the RP lifetime, the excitation pulse can be regarded as a delta-function, ensuring that no nuclear spin polarization can be built up due to multiple turnovers during excitation [22]. Since the average turnover-rate is smaller than 2 s^{-1}, the nuclear spin relaxation time in the RC ground state has to be considerably slower,

while concomitantly in the $^3P^*$ state it has to be of the order of the triplet lifetime to build up a steady-state nuclear spin polarization. Preliminary checks show no changes in the experimental data when the repetition rate of excitation is changed to 0.02 Hz, indicating that nuclear spin relaxation in the ground state is much slower than 50 s, much faster than 0.07 s or does not accumulate at all.

The radical pair lifetime and triplet yields

The absorption change ΔA_P consists of a bleaching due to the contributions of both P^+BH^- and $^3P^*$. At time delay $t = 0$, only P^+BH^- contributes to ΔA_P and decays completely with the RP lifetime τ_{RP}. At long delay times the long-lived $^3P^*$ states remain, again bleaching the PBH ground-state absorption. The triplet yield is expected to evolve approximately as the decay product of an exponentially decaying parent. Thus we fit our data to the relation

$$\Delta A_P(t) = \Delta A_0[e^{-t/\tau_{RP}} + \Phi_T(1-e^{-t/\tau_{RP}})] + \Delta A_Q \qquad (5)$$

where Φ_T is the final triplet yield, ΔA_0 the absorption change at $t = 0$ for the RCs not containing ubiquinone and ΔA_Q is the extrapolated absorption change at $t = 0$ for the quinone-containing part of the RCs. In order to avoid overlap effects with the excitation pulse, we consider only those data starting at 3 ns delay time. Due to the quantum mechanical nature of singlet–triplet mixing, small oscillations are expected to be superimposed on the exponential decay of the RP as well as on the triplet evolution, reflecting the quantum beats between the singlet and the triplet radical pair states. Such deviations, however, are expected to be small, since $k_T \gg k_S$ and $k_T \gg$ HFI throughout the temperature range, as we will see later. Once in the triplet state, the RPs have little chance to recombine into the singlet state. The coherent quantum mechanical spin motion is damped very quickly, since the stochastic recombination process dominates HFI. Finally, the large amount of different hyperfine couplings lead to rapid dephasing of the various oscillatory contributions. Only at the very beginning of the triplet evolution a slight lag is expected, since singlet–triplet mixing starts quadratically with time [23]. We have checked these assumptions experimentally by probing the triplet evolution directly in the isosbestic points of the RP difference spectrum at 533 and 552 nm. Except for the expected delay in the onset of triplet evolution at very early times (< 3 ns), the measured kinetics are consistent with the model implicit in Eqn. 5. This is another reason why we dismissed data at very early times from the fit. We attained similar results with measurements in the Q_x band of H at 543 nm, although with somewhat poorer accuracy due to the smaller absorption change in this band.

The RP lifetimes, τ_{RP}, are listed in Table IA, the triplet yields in Table IB. For comparison, at room temperature, lifetimes of 13 ns (0 G) and 17 ns (1 kG) have been reported [25,26]; the room temperature triplet yield is also in good agreement with previous values [25,26]. Data presented in Ref. 27 partially agree, with considerable deviation, however, in the high-field lifetime (22 ns) and the low-field triplet yield (47% compared to 30%).

The recombination rates k_S and k_T

In order to analyse the magnetic-field-dependent $^3P^*$ lifetimes, $1/k_{OBS}$, we need information about k_S and k_T. From the analysis of the lifetime broadening of the RP state (as reflected in the half-width at half-maximum (HWHM) of the magnetic field dependence of the triplet yield of room temperature data [26]) we know that at least one of the recombination rates is about $(3–6) \cdot 10^8$ s^{-1}. Since the inverse RP lifetimes are considerably smaller than this value, a bottleneck has to be effective in this RP decay channel. Apparently, the hyperfine-induced singlet–triplet mixing constitutes this bottleneck and identifies the triplet recombination rate, k_T, as responsible for the lifetime broadening. Since a magnetic field reduces HFI-induced singlet–triplet mixing, the RP lifetime is expected to increase or decrease, respectively if the triplet channel is faster or slower than the singlet channel [28,29]. An increase in the RP lifetime in quinone-depleted RCs at moderate magnetic fields (about 1 kG) was observed at room temperature [25,26] and at low temperatures [27], corroborating $k_T > k_S$. The same conclusion was drawn for quinone-reduced RCs [29,30].

Low-temperature measurements of the magnetic field dependence of the triplet yield, as re-

flected in the absorption changes 44 ns after excitation at 543 nm, showed an almost constant width of the singlet–triplet resonance as a function of temperature [10], increasing by ≈ 10 G between 295 and 90 K. As discussed previously [10], such an increase points to a slight increase of k_T with decreasing temperature, as is expected for activationless electron transfer [31]. An increased HWHM of the magnetic field dependence of the triplet yield can principally result from increased exchange interaction as well. Simulation, however, discard this possibility, since in this case the maximum triplet yield should occur at nonzero magnetic fields [10]. Even more clearly RYDMR spectra show an impressive temperature independence of the exchange interaction [32]. We performed improved measurements of the magnetic field dependence of the triplet yield probing changes in

TABLE I

TEMPERATURE-DEPENDENT RADICAL PAIR (RP) LIFETIMES, TRIPLET YIELDS, ELECTRON TRANSFER RATES INVOLVED IN RECOMBINATION DYNAMICS, INTERSYSTEM CROSSING RATE $^3P^* \rightarrow P$ AND FREE ENERGY DIFFERENCE, $\Delta G(RP - {}^3P^*)$.

A: RP lifetime obtained from Eqn. 5

B: Triplet yields obtained from transient absorption measurements at 880 nm as described.

C: Singlet recombination rates k_S calculated according to Eqn. 6.

D: Triplet decay rates from Ref. 18.

E: Triplet charge separation rate k_{-T},

(a) calculated from Eqn. 2 with no account for inhomogeneous distribution of RCs with respect to HFIs.

(b) allowing for very slow nuclear spin relaxation compared to k_{OBS}.

(c) assuming very fast nuclear spin relaxation compared to k_{OBS}.

F: Intersystem crossing rate; (a), (b) and (c) as in E.

G: Free enthalpy difference $\Delta G(RP - {}^3P^*)$ from E according to Eqn. 9; (a), (b) and (c) as in E.

T(K):	290	270	250	230	185	90
A Radical pair lifetimes						
τ_{RP}(0 G) [ns] ± 8%	13.0	13.7	15.0	16.4	18.1	21.2
τ_{RP}(700 G) [ns] ± 8%	15.8	16.9	18.1	21.3	23.2	34.3
B Triplet yields						
Φ_T(0 G) ± 0.02	0.30	0.31	0.34	0.39	0.45	0.71
Φ_T(700 G) ± 0.02	0.19	0.20	0.24	0.27	0.36	0.52
C Singlet recombination rates (total)						
k_S(0 G) [10^7 s^{-1}] ± 0.6	5.8	5.4	4.8	4.0	3.3	1.5
k_S(700 G) [10^7 s^{-1}] ± 0.6	5.3	4.9	4.4	3.6	2.9	1.5
D Triplet decay rates						
k_{OBS}(0 G) [10^4 s^{-1}]	1.96	1.55	1.28	1.06	0.86	0.73
k_{OBS}(1 kG) [10^4 s^{-1}]	1.48	1.32	1.12	0.99	0.84	0.72
E Triplet charge separation rate						
(a) k_{-T} [10^5 s^{-1}] ± 30%	7.1	3.7	3.1	2.0	0.48	
(b) k_{-T} [10^5 s^{-1}] ± 30%	4.1	2.1	1.6	0.9	0.20	
(c) k_{-T} [10^5 s^{-1}] ± 30%	3.3	1.6	1.2	0.6	0.14	
F Intersystem crossing rate						
(a) k_{ISC} [10^3 s^{-1}] + 30%	6.5	9.0	7.4	7.9	7.9	
(b) k_{ISC} [10^3 s^{-1}] ± 30%	9.6	10.5	9.2	8.7	8.2	
(c) k_{ISC} [10^3 s^{-1}] ± 30%	12.9	12.2	10.5	9.5	8.3	
G Free enthalpy difference $\Delta G(RP - {}^3P^*)$						
(a) ΔG [eV] ± 0.008	0.151	0.156	0.148	0.147	0.143	
(b) ΔG [eV] ± 0.008	0.165	0.169	0.163	0.161	0.153	
(c) ΔG [eV] ± 0.008	0.171	0.176	0.169	0.168	0.159	

the Q_y absorption band of P at considerably longer delay times (92 ns), confirming that $k_T = (3\text{–}6) \cdot 10^8\ s^{-1}$ [10].

As shown previously [23], the RP lifetime can be calculated from

$$\tau = \frac{\Phi_S}{k_S} + \frac{\Phi_T}{k_T} \tag{6}$$

Eqn. 6 is the basis for the determination of k_S. Because of the singlet–triplet mixing constituting the bottleneck in $^3P^*$ formation, the triplet yield is smaller with respect to the recombination rate, k_T, than the singlet yield with respect to k_S. Therefore, the RP lifetime is closely connected to the decay rate, k_S, in the singlet decay channel, and the contribution of the second term in Eqn. 6 is small. The rate k_S calculated from Eqn. 6 and the data given in Table IA and B are listed in Table IC using $\Phi_S + \Phi_T = 1$. The rates obtained from the measurements at high and low field are fairly consistent. The room temperature value of k_S obtained from Eqn. 6 is in good agreement with the value $k_S = 5.6 \cdot 10^7$ [26] obtained from a more rigorous analysis involving the explicit numerical solution of the stochastic Liouville equation, and its fit to a complete set of magnetic-field- and time-dependent data at room temperature. The small temperature-dependence of τ refects the small temperature-variation of k_S. The apparent activation energy for k_S in this temperature range is 0.014 eV, somewhat smaller as the one deduced in Ref. 27. Such weak temperature-dependence can be expected for electron transfer reactions in the inverted regime involving free energy changes larger than the reorganization energy [33].

Since k_S might have a temperature-activated contribution from recombination via the $^1P^*$ state, this contribution in principle might be responsible for the temperature dependence of the overall rate. The overall singlet recombination rate, k_S, is composed of the rate of direct recombination into the ground state, ^dk_S, and of an effective rate k_S^{eff}. This arises from the recombination into the $^1P^*$ state with the rate k_{-1}, of which a small part subsequently decays into the PBH ground state with the rate k_0, while the vast majority undergoes renewed charge separation, with the rate k_1, k_1 exceeds k_0 by at least 10^2 as known from the high quantum yield of charge separation [34]. If k_{-1} is large enough, hopping of the electron between the states $^1P^*$ and P^+BH^- results before the RP decays. Such a process can severely disturb the spin-dependent recombination dynamics and can best be handled in a model introduced to describe hopping between two states with different spin–spin exchange interactions at the two sites [35]. Replacing the state associated with the 'close' site in Ref. 35 (i.e., the one with the large exchange interaction) with $^1P^*$, makes the problems discussed here and in Ref. 35 isomorphous. According to Eqn. 2.11 in Ref. 35, the effective singlet recombination rate is given by:

$$k_S^{eff} = k_{-1} \frac{k_0}{k_1 + k_0} \tag{7}$$

i.e., k_{-1} weighted with the probability of deactivating into the ground state rather than carrying out renewed charge separation to form P^+BH^-. For the overall recombination rate we obtain:

$$k_S = {}^dk_S + k_{-1}(1 - \Phi_{CS}) \tag{8}$$

with Φ_{CS} being the quantum yield for a single charge separation act forming P^+BH^-. Φ_{CS} is at least as large as the quantum yield of P^+BHQ^- formation, which was determined to be larger than 0.98 [34]. A hopping process as described above would also lead to a broadening of the HWHM of the magnetic field dependence of the triplet yield [26,35], if k_{-1} were larger than k_T. From Eqn. 9 we can get an even lower boundary for k_{-1}. Taking $k_1 = 3.57 \cdot 10^{11}\ s^{-1}$ and $\Delta G(^1P^*\text{–}RP) = 0.26$ eV [17], we get $k_{-1} < 9 \cdot 10^6\ s^{-1}$ for quinone-depleted RCs. Accordingly, only a negligible fraction of $4 \cdot 10^{-3}$ of the RPs recombines to the ground state via $^1P^*$. Therefore, this contribution cannot be responsible for the observed temperature variation of k_S. Since Φ_{CS} is not expected to decrease at low temperatures because of the activationless nature of k_1 [4], this fraction is considerably smaller at low temperatures due to the reduction in k_{-1}.

The analysis of the quantum yield of fluorescence and triplet formation of whole cells of *Rb.*

sphaeroides 2.4.1 [36] under reducing conditions led to $k_{-1} = (4.3\text{–}8) \cdot 10^8\ s^{-1}$, a value which is larger by almost two orders of magnitude than the one considered here for quinone-depleted RCs. In this case, up to 28% of the singlet recombination is considered to proceed via the $^1P^*$ state. The free energy difference of $\Delta G(^1P^* - RP) = 0.045\text{–}0.075$ eV implicit in these data is much smaller than the one derived from time-resolved fluorescence data for reduced RCs [37,38] or the one derived in this paper for quinone-depleted RCs.

Kinetics and energetics associated with $[P^+BH^-]$ and $^3P^*$

The charge separation rate k_{-T}

Inverse lifetimes of the triplet state $^3P^*$ at magnetic fields of 0 G and 1 kG were extracted from Fig. 3 in Ref. 16 and are listed in Table ID for various temperatures. Table IE,a shows the charge separation rate k_{-T} calculated from the magnetic field modulation of the $^3P^*$ lifetime according to Eqn. 2, thus neglecting an inhomogeneous distribution of RCs with respect to the effective HFIs. Experimental triplet yields obtained at 700 G were put together with triplet lifetimes determined at 1 kG. This is certainly justified because the triplet yield is expected to be constant in this magnetic field range, since Zeeman splitting by far exceeds the hyperfine interaction and additional singlet–triplet mixing due to differences in g value of the two radicals is not yet significant. At 90 K, k_{-T} cannot be evaluated, since the change of k_{OBS} with the magnetic field is too small.

In order to test the consistency of the obtained data, we calculate the intersystem crossing rate k_{ISC} from Eqn. 1. As shown in Table IF,a, k_{ISC} is almost constant with temperature, the low-temperature value coinciding with the value given in Ref. 16.

The rate k_{-T} obtained when nuclear spin distribution is accounted for is shown in Table IE,b and E,c for the case of slow and fast nuclear SLR, respectively. These data differ only slightly from the ones obtained from Eqn. 2, qualifying Eqn. 2 as a good working hypothesis. The true value for k_{-T} has to be within the limits given by the two extreme cases of nuclear spin relaxation. Since nuclear spin relaxation in general is considerably slower than k_{OBS}, we would favour the values given in Table IE,b. However, the influence of SLR on the data is smaller than the uncertainty of measurement. Thus, there remains no ambiguity of the data concerning SLR. We also calculated the accompanying intersystem crossing rates (Table IF,b and c) which again change only slightly for the two cases, and are quite temperature-independent.

Surprisingly, the triplet decay rate, k_{DEC}, of RCs in which the quinone has been reduced is larger by a factor of 10 at room temperature than for quinone-depleted ones [16,39], and reveals no magnetic field dependence [16]. At low temperatures the triplet decay rate is the same for quinone-depleted and quinone-reduced RCs. At higher temperatures it exhibits a larger apparent activation energy of 0.095 eV [39] for quinone-reduced samples. Can this change reflect a change of the free enthalpy gap $\Delta G(RP - {}^3P^*)$? In fact, one would expect a shift of the state P^+BH^- to somewhat higher energies due to the Coulomb interaction with the additional charge on the quinone [37,38], thus reducing k_{-T}. Neither of the other contributions to k_{DEC} could compensate for this decrease of k_{-T} in order to account for increasing k_{DEC}: k_S and k_T differ only slightly for both preparations due to the similarity in the HWHM and of the radical pair lifetimes [Ogrodnik et al., unpublished results] and the triplet yield even decreases by more than a factor of two [27,30]. From these findings and Eqn. 2 one might expect $k_{DEC}(0\ G) - k_{DEC}(1\ kG)$ to be similar for samples with reduced quinone and samples depleted of quinone, i.e., $k_{DEC}(0\ G) - k_{DEC}(1\ kG) \approx 5 \cdot 10^3\ s^{-1}$ also for reduced RCs at 295 K. Since k_{DEC} of reduced RCs is 10-times larger than that of RCs depleted of quinone, the magnetic-field-dependent change in k_{DEC} will amount to less than 3% at room temperature, the effect being beyond the resolution of the experiment [16]. Thus, the apparent absence of a magnetic field effect on the triplet lifetime can well be understood. In other words, the overwhelming part of the $^3P^*$ decay does not occur via the RP state. It is not magnetic-field-dependent and is comprised in the rate $k_{isc} \approx k_{DEC}$. It is this part of the observed triplet decay rate which is responsible for the

increase in the apparent activation energy, and not as one might expect the term due to the decay via the radical pair state. Because of the large energy splitting between $^1P^*$ and $^3P^*$, an enhancement of k_{isc} due to the fast relaxing Fe^{2+} is not expected, in particular because the recombination dynamics of the RP, exhibiting only extremely small energy splittings, seem to be almost unaffected by the presence of Fe^{2+} in reduced RCs. Thus, the mechanism of enhancement of k_{isc} in reduced RCs remains veiled.

Change in free energy

In lines G,a, G,b and G,c of Table I the change in free energy $\Delta G(RP-{}^3P^*)$ as a function of temperature is calculated from

$$k_{-T} = k_T \exp(-\Delta G/k_B T) \quad (9)$$

and the corresponding line of Table IE. Due to the logarithmic dependence on k_{-T}, the differences in ΔG are very small and within the error of measurement for the cases (b) and (c). It should be noted that these values do not depend on k_T, since k_T cancels in Eqns. 2 and 9 *. In the other cases we explicitly calculated k_{-T} to be twice as large as indicated in line E,b or E,c of Table I, if we double the value of k_T. The small reduction of $\Delta G(RP-{}^3P^*)$ with temperature (295–185 K) by an amount of 0.011 ± 0.015 eV (slow nuclear spin relaxation) and 0.012 ± 0.015 eV (fast spin relaxation) is almost within the uncertainty of the determination. Since spin relaxation is expected to be slower than k_{OBS}, we will refer to the values in Table IG,b in the following, employing a room temperature value of $\Delta G(RP-{}^3P^*) = 0.165 \pm 0.008$ eV.

Evaluation of the energy difference $\Delta H(RP-{}^3P^*)$ from the temperature dependence of k_{OBS} [16] could not account for temperature-dependent changes of the parameters involved in Eqn. 1. We have recalculated ΔH (and the entropy change ΔS) from the new experimental data. Assuming ΔH and ΔS to be temperature independent, a linear regression to the temperature-dependent data would give an estimate of the energy difference and the entropy difference for the three cases:

(a) $\Delta H(RP-{}^3P^*) = 0.123 \pm 0.05$ eV

$\Delta S(RP-{}^3P^*) = -(1.05 \cdot 10^{-4} \pm 1.5 \cdot 10^{-4})$ eV/K.

(b) $\Delta H(RP-{}^3P^*) = 0.130 \pm 0.05$ eV

$\Delta S(RP-{}^3P^*) = -(1.32 \cdot 10^{-4} \pm 1.5 \cdot 10^{-4})$ eV/K.

(c) $\Delta H(RP-{}^3P^*) = 0.137 \pm 0.05$ eV

$\Delta S(RP-{}^3P^*) = -(1.29 \cdot 10^{-4} \pm 1.5 \cdot 10^{-4})$ eV/K.

The ΔH values are in agreement with Ref. 16. The values for the entropy change upon charge separation from $^3P^*$ are negligible within the uncertainty of measurement. In any case, it is considerably smaller than the one obtained for charge separation from $^1P^*$: $\Delta S(RP-{}^1P^*) = 6.5 \cdot 10^{-4}$ eV/K deduced from temperature-dependent fluorescence data from RCs containing reduced quinone [38] and even opposite in sign. Discussing models of primary electron transfer, it seems justified to neglect the entropy contribution and regard $\Delta G(RP-{}^3P^*) \approx \Delta H(RP-{}^3P^*)$.

Comparison with data from delayed fluorescence and phosphorescence measurements

From the temperature dependence of the μs-delayed fluorescence, $\Delta H({}^1P^*-{}^3P^*) = 0.4$ eV was deduced [19]. Phosphorescence of the $^3P^*$ state has recently been detected at 1317 nm independently of temperature [20]. Together with the fluorescence peaks at 913 and 925 nm for 295 and 90 K, respectively [38], estimates of $\Delta H({}^1P^*-{}^3P^*) \approx 0.42$ and 0.40 eV can be made, being almost independent of temperature.

Time-resolved fluorescence measurements have been performed on quinone-depleted RCs with subnanosecond [18] and nanosecond [17] time resolution yielding free energy differences of $\Delta G({}^1P^*-RP) = 0.148$ and 0.26 eV, respectively. However, these free energy gaps refer to two different

* According to Eqn. 6, k_s has a contribution from k_T, which does not cancel. This contribution can be calculated to be less than 40% (using the high-field data, Table I), being considerably smaller than the uncertainty of measurement, and is therefore neglected.

states since different kinetic models have been invoked in the analyses [38,40]. The smaller value pertains to a postulated non-relaxed RP state, while the larger one refers to the relaxed RP state with a lifetime in the 10 ns range which gives rise to magnetic-field-dependent recombination dynamics and which is relevant for the decay of $^3P^*$. It can be shown that $\Delta G(^1P^* - RP_{relaxed})$ can be extracted from the ratio of the quantum yields of the fastest (prompt) and the slowest fluorescence components (Ogrodnik, A, unpublished results), independently of which model is used to interpret one or more non-understood intermediate fluorescence components. This holds even if any of the intermediate fluorescence components turns out to be a preparational artifact. In particular, since neither the fastest nor the slowest components are expected to be distorted by background fluorescence of damaged RCs or free pigments, our analysis is insensitive to these kinds of artifacts, in contrast to the one carried out in Ref. (18,38). Such an analysis of data taken from Ref. 18 yields $\Delta G(^1P^* - RP) = 0.245$ eV, in good agreement with Ref. 17.

Together with $\Delta G(RP - {}^3P^*) = 0.165$ eV we get $\Delta G(^1P^* - {}^3P^*) = 0.410$–$0.425$ eV at room temperature. Comparing this value with the phosphorescence data yielding $\Delta H(^1P^* - {}^3P^*) = 0.42$ [20], we recognize that $\Delta G(^1P^* - {}^3P^*) \approx \Delta H(^1P^* - {}^3P^*)$, indicating that $^1P^*$ and $^3P^*$ are similar in entropy. Note that the slight decrease in $\Delta G(RP - {}^3P^*)$ with temperature is also accompanied by a corresponding decrease in $\Delta H(^1P^* - {}^3P^*)$. Since $\Delta G(RP - {}^3P^*)$ has only little entropy contribution, the entropy change between $^1P^*$ and RP has to be small, implying $\Delta G \approx \Delta H$ for all combinations of states $^1P^*$, RP and $^3P^*$ in quinone-depleted RCs. In conclusion, we propose for RCs of *Rb. sphaeroides* the following energy parameters at room temperature [41]:

$$\Delta G(^1P^* - RP) \simeq \Delta H(^1P^* - RP) = 0.245\text{–}0.26 \text{ eV}$$

$$\Delta G(RP - {}^3P^*) \simeq \Delta H(RP - {}^3P^*) = 0.165 \text{ eV}$$

$$\Delta G(^1P^* - {}^3P^*) \simeq \Delta H(^1P^* - {}^3P^*) = 0.42 \text{ eV}$$

These values seem to be suited as a basis for the analysis of the various models for the primary electron transfer processes in RCs.

Acknowledgements

We thank Dr. E.W. Knapp as well as our collaborators U. Eberl and Dr. W. Lersch for fruitful discussions of the results. Financial support from the Deutsche Forschungsgemeinschaft (Sonderforschungsbereich 143) is gratefully acknowledged.

References

1 Martin, J.-L., Breton, J., Hoff, A.J., Migus, A. and Antonetti, A. (1986) Proc. Natl. Acad. Sci. USA 83, 957–961.
2 Woodbury, N.W., Becker, M., Middendorf, D. and Parson, W.W. (1985) Biochemistry 24, 7516–7521.
3 Breton, J., Martin, J.-L., Petrich, J., Migus, A. and Antonetti, A. (1986) FEBS Lett. 209, 37–43.
4 Martin, J.-L., Breton, J., Lambry, J.C. and Fleming, G.R. (1988) in Reaction Center – Structure and Dynamics, NATO ASI Series, Series A: Life Sciences, Vol. 149 (Breton, J. and Verméglio, A., eds.), pp. 195–203, Plenum Press, New York.
5 Allen, J.P., Feher, G., Yeates, T.O., Rees, D.C., Deisenhofer, J., Michel, H. and Huber, R. (1986) Proc. Natl. Acad. Sci. USA 83, 8586–8593.
6 Chang, C.H., Tiede, D., Tang, J., Smith, U., Norris, J.R. and Schiffer, M. (1986) FEBS Lett. 205, 82–86.
7 Allen, J.P., Feher, G., Yeates, T.O., Komiya, H. and Rees, D.C. (1987) Proc. Natl. Acad. Sci. USA 84, 5730–5734.
8 Hoff, A.J. (1981) Q. Rev. Biophys. 14, 599–665.
9 Hoff, A.J. (1986) Photochem. Photobiol. 43, 727–745.
10 Ogrodnik, A., Remy-Richter, N., Michel-Beyerle, M.E. and Feick, R. (1987) Chem. Phys. Lett. 135, 576–581.
11 Marcus, R.A. (1987) Chem. Phys. Lett. 133, 471–477.
12 Fischer, S.F. and Scherer, P.O.J. (1987) Chem. Phys. 115, 151–158.
13 Bixon, M., Jortner, J., Michel-Beyerle, M.E., Ogrodnik, A. and Lersch W. (1987) Chem. Phys. Lett. 140, 626–630.
14 Bixon, M., Jortner, J., Plato, M. and Michel-Beyerle, M.E. (1988) in Reaction Center – Structure and Dynamics, NATO ASI Series, Series A: Life Sciences, Vol. 149 (Breton, J. and Verméglio, A., eds.), pp. 399–420, Plenum Press, New York.
15 Parson, W.W. and Warshel, J. (1987) J. Am. Chem. Soc. 109, 6143–6152.
16 Chidsey, E.D., Takiff, L., Goldstein, R.A. and Boxer, S.G. (1985) Proc. Natl. Acad. Sci. USA 82, 6850–6854.
17 Hörber, J.K.H., Göbel, W., Ogrodnik, A., Michel-Beyerle, M.E. and Cogdell, R.J. (1986) FEBS Lett. 198, 273–278.
18 Woodbury, N.W., Parson, W.W., Gunner, M.R., Prince, R.C. and Dutton, P.L. (1986) Biochim. Biophys. Acta 851, 6–22.
19 Shuvalov, V.A. and Parson, W.W. (1981) Proc. Natl. Acad. Sci. USA 78, 957–961.
20 Takiff, L. and Boxer, S. (1987) Photochem. Photobiol. 45, Suppl. 61S.

21 Schulten, K. and Wolynes, P.G. (1978) J. Chem. Phys. 68, 3292–3297.
22 Goldstein, R.A. and Boxer, S.G. (1987) Biophys. J. 51, 937–946.
23 Haberkorn, R. and Michel-Beyerle, M.E. (1979) Biophys. J. 26, 489–498.
24 Boxer, S.G., Chidsey, C.E.D. and Roelofs, M.G. (1982) Proc. Natl. Acad. Sci. USA 79, 4632–4636.
25 Chidsey, C.E.D., Kirmaier, C., Holten, D. and Boxer, S.G. (1984) Biophys. Acta 424–437.
26 Ogrodnik, A., Krüger, H.W., Orthuber, H., Haberkorn, R., Michel-Beyerle, M.E. and Scheer, H. (1982) Biophys. J. 39, 91–99.
27 Budil, D.E., Kolaczkowski, V., and Norris, J.R. (1987) in Progress in Photosynthesis Research (Biggins, J., ed.), Vol. I, pp. 245–248, Martinus Nijhoff, Dordrecht.
28 Michel-Beyerle, M.E., Scheer, H., Seidlitz, H. and Tempus, D. (1979) FEBS Lett. 100, 9–12.
29 Michel-Beyerle, M.E., Scheer, H., Seidlitz, H. and Tempus, D. (1980) FEBS Lett. 110, 129–132.
30 Schenk, C.C., Blankenship, R.E. and Parson, W.W. (1982) Biochim. Biophys. Acta 680, 44–59.
31 Bixon, M. and Jortner, J. (1986) J. Phys. Chem. 90, 3795–3800.
32 Hunter, D.A., Hoff, A.J. and Hore, P.J. (1987) Chem. Phys. Lett. 134, 6–11.
33 Marcus, R. and Sutin, N. (1985) Biochim. Biophys. Acta 811 265–322.
34 Wraight, C.A. and Clayton, R.K. (1974) Biochim. Biophys. Acta 33, 246–260.
35 Haberkorn, R., Michel-Beyerle, M.E. and Marcus, R.A. (1979) Proc. Natl. Acad. Sci. USA 76, 4185–4188.
36 Rademaker, H. and Hoff, A.J. (1981) Biophys. J. 34, 325–342.
37 Hörber, J.K.H., Göbel, W., Ogrodnik, A., Michel-Beyerle, M.E. and Cogdell, R.J. (1986), FEBS Lett. 198, 268–272.
38 Woodbury, N.W.T. and Parson, W.W. (1984) Biochim. Biophys. Acta 767, 345–361.
39 Shuvalov, V.A. and Parson, W.W. (1981) Biochim. Biophys. Acta 638, 50–59.
40 Hörber, J.K.H., Göbel, W., Ogrodnik, A., Michel-Beyerle, M.E. and Knapp, E.W. (1985) in Antennas and Reaction Centers of Photosynthetic Bacteria-Structure, Interactions and Dynamics (Michel-Beyerle, M.E., ed.), p. 292, Springer Verlag, Berlin.
41 Ogrodnik, A., Volk, M. and Michel-Beyerle, M.E. (1988) in Reaction Center – Structure and Dynamics, NATO ASI Series, Series A: Life Sciences, Vol. 149 (Breton, J. and Verméglio, A., eds.), pp. 177–184, Plenum Press, New York.